Computational Tools and Data and its Application to Materials Design Based on Failure Physics

David Linder[1], Carl-Magnus Lancelot[2], Ida Berglund[1], Anders Engström[2]
[1]QuesTek Europe AB
Råsundavägen 18, 16967 Solna
SWEDEN

[2]Thermo-Calc Software AB
Råsundavägen 18, 16967 Solna
SWEDEN

Corresponding author: anders@thermocalc.com

Keywords: AVT-356 Research Symposium, Materials design, Computational thermodynamics, Creep performance, Superalloy, Thermo-Calc Software

ABSTRACT

This paper presents how CALPHAD-based (CALculation of PHAse Diagrams) computational tools included in the Thermo-Calc software suite can be used for microstructure modelling, and how performance can be predicted with the intelligent use of microstructure modelling, existing property models and experimental data within an Integrated Computational Materials Engineering (ICME) framework. This framework allows to move beyond empirical modelling and data fitting. Exemplified is creep performance of Ni-based superalloy 718 (IN718). The Thermo-Calc Precipitation module (TC-PRISMA) is used together with experimental data from literature, to simulate the manufacturing of IN718 and its in-service use, via γ' and γ'' precipitation modelling during two-stage annealing, and coarsening during long-term heat treatment at 600 and 800 °C, respectively. With this microstructure input, strength is predicted. Combined, these predictions are used for creep rate predictions across time, temperature and load, simulating in-service behavior of e.g., an aeroengine disk. Overall, we show that, by coupling existing data, models and metallurgical knowledge, CALPHAD-based predictions allow not only to evaluate properties, such as creep, to understand sensitivity within a well-studied composition range, but also to explore novel chemistries and ultimately design alloys for improved performance.

1.0 INTRODUCTION

To ensure the ability to make performance driven design of components and the optimization of material-specific requirements, we need to be able to measure, analyse and replicate the changes in material properties during service. To achieve this, we need to understand the process-structure-property relationships of the materials, as highlighted in the publication of the National Academies Report on ICME in 2008.

The Materials Innovation Infrastructure outlined in the Materials Genome initiative report published in 2011 also highlights the synergy between measured (experimental and physical test data), computational models (simulation) and data repositories. Indeed, to perform simulations with the objective to predict performance and to make lifetime predictions, requires good materials data.

A challenge is that the properties of materials depend on both their chemical composition and processing conditions, as well as service conditions. Handbook data and data repositories alone tend to be limited in the scope of materials covered (their compositions) or the temperature ranges (processing conditions) or

lack of time dependence. As such, the engineering simulations which depend on these data are limited, especially for cases involving novel materials and often it becomes necessary to go and measure the needed data or accept the uncertainty.

The calculation of phase diagrams was realized by J. W. Gibbs (Gibbs, 1873) as a novel graphical tool, useful to describe the changing of thermodynamic states of a system, and has become a crucial element in the design of new materials. Today, the CALPHAD method involves the use of sophisticated computational tools to evaluate the thermodynamic properties and phase diagrams of materials (Lukas, Fries and Sundman, 2007). The strength of the method lies in the possibility to predict properties of complex alloys such as Ni-base superalloys, based on thermodynamic descriptions of lower-order systems such as binary, ternary and quaternary systems. The properties of a higher-order alloy are interpolated between, or extrapolated from, the description of the lower-order systems. The CALPHAD approach captures the composition and temperature dependence of properties, as well as their temporal evolution, for industrial multi component alloys. As such, data can be simulated for materials or conditions where there are gaps in the measured data. Additionally, location specific properties can be predicted and optimized for a part, which means that manufacturers will no longer be restricted to design minimums.

CALPHAD predictions can be used to complement database repositories of measured data, improve machine learning models, and can also be used as input into engineering codes that require more robust materials property data. Further, coupling measured data and the current understanding of failure physics with the intelligent use of CALPHAD-based predictive process-structure and structure-property models, enables computational evaluation and design of novel materials and optimized in-service performance. Additionally, critical knowledge gaps and associated need for new measured data can be identified in this ICME process, to ultimately both improve the understanding of specific failure physics and reduce the uncertainty of the simulations.

In this paper, IN718 is used as an example to showcase the capabilities of an ICME framework incorporating CALPHAD tools, databases and mechanistic models to predict the in-use properties and performance of aeroengine materials. Specifically, strength and creep are predicted as function of microstructure evolution at elevated temperature, connecting microstructure evolution with component life. Furthermore, the potential for performance enhancement based on chemistry modification or alloy design is shown using computational materials design.

These results show that although commonly used handbook parameters and single-value fitting of composition-dependent parameters have been successful in capturing the effect of variations in temperature and applied stress on creep rate, this is highly dependent on available experimental data for a specific composition. The extended use of CALPHAD-based predictions in an ICME framework, to not only include microstructure evolution over time, but also for determination of parameters such as the vacancy diffusivity, enables an additional dimension of uncertainty quantification in the creep performance predictions, as well as extrapolation of well-established creep models beyond the specific composition range they were calibrated for. As the CALPHAD approach matures for Structure–Properties relations, it becomes possible to move beyond the traditional approach, where model parameters are treated as fitting parameters.

2.0 METHODOLOGY

The properties, and by extension the performance, of any alloy is dictated by the chemistry and microstructure. Therefore, it is important to understand and predict the evolution of these phases across time and temperature, in order to predict component in-service performance. We know from decades of research and testing, and metallurgical understanding, that creep is controlled by diffusion, dislocation glide and climb, grain boundary sliding and particle shearing or bowing. For superalloys used in aeroengines, and for alloy 718 in particular, the performance limiting mechanisms are closely connected to the precipitate type,

volume fraction and size. The main strengthening precipitate in IN718 is the metastable Ni3Nb phase (γ'') (Drexler *et al.*, 2015) which transforms to the stable Ni3Nb (δ) phase after long-term exposure at elevated temperatures, especially above 850 ºC (Liu, Yao and Chen, 1999). At lower temperatures and shorter exposure time, the mechanical properties of the alloy evolve primarily due to the precipitation, coarsening and dissolution of the γ'' phase, depending on the thermal history of the material. According to recent work (Malmelöv *et al.*, 2020), dislocation climb is the dominating mechanism up to around 750- 800 ºC. A semi-empirical creep model was selected to incorporate the influence of precipitate size and volume fraction on these mechanisms. Property predictions were then made by incorporating CALPHAD-produced data into selected variables of the models. Unlike empirical modelling or fitting parameters for the mechanistic models to experimental creep data, CALPHAD-based predictions allow for extrapolation to compositions, temperatures and timescales outside well-established systems. Furthermore, the physical basis of the parameters determined through the CALPHAD-based approach enables not only short-term creep performance, but also allows for predictive modelling of the influence of long-term microstructure evolution and the corresponding effects on component lifetime.

An ICME framework based on known process-structure and structure-property relations, such as established metallurgical understanding and pre-existing data and models, is used for modelling the creep behaviour of IN718. In this work, we model the microstructure of the material (matrix, precipitates size and volume fraction) and feed directly into a strength model, then further into the creep rate model. An overview of the calculation flow highlighting the CALPHAD-based parameter determination for the property models is shown in Figure 1. This creep modelling framework builds upon input from thermodynamic and kinetic simulations and a strength model which are all functions of composition, temperature and time.

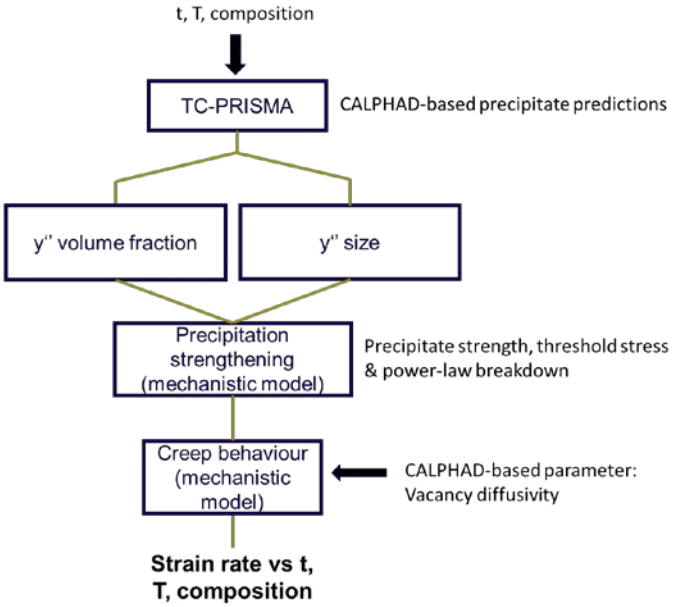

Figure 1: Schematic calculation flow used in the ICME framework for creep performance predictions, including CALPHAD-based parameter determination for mechanistic structure-property models

2.1 Creep modelling

In this work we utilize a creep model that captures the influence of temperature and applied stress on the creep rate. The power-law creep model proposed by Li and Langdon (Li and Langdon, 1997) incorporating the

threshold-stress concept (Wilshire, B.; Evans, 1985) in the form proposed by Heilmaier and Reppich (Heilmaier and Reppich, 1999), is here used in the modified sinh-form, similar to that used by Drexler et al. (Drexler *et al.*, 2018), for applicability beyond the power-law creep regime. The creep rate, $\dot{\varepsilon}$, is here given by:

$$\dot{\varepsilon} = A\frac{D_{vac}\mu_T b}{k_B T} sinh(P\frac{\sigma_{eff}}{\mu_T})^n \qquad (1)$$

Where A is a dimensionless material-dependent parameter, D_{vac} (m2/s) is the vacancy diffusivity, μ_T (GPa) is the alloy shear modulus, b is the Burgers vector, k_B (J/K) is the Boltzmann constant, σ_{eff} (MPa) is the effective creep stress, n is the creep exponent, and P is a power-law breakdown parameter which is related to the strength of the alloy.

The creep model established on a physical basis becomes industrially useful only when the model parameters, such as vacancy diffusivity and lattice mismatch, are determined in the multidimensional composition space. The CALPHAD approach, originally for bulk thermodynamics, has been extended to cover thermophysical properties related to kinetic phenomena and crystal defects which governs deformation and failure. Therefore, the CALPHAD approach enables an increasingly reliable connection between mechanistic modelling of creep and industrially relevant alloy compositions.

To predict the creep rate, we take physical constants from CALPHAD tools or handbook data, and the diffusivity and strength from separate science-based models and microstructure evolution predictions from CALPHAD. Drexler et al. emphasize the importance of accurate description of threshold stress and microstructure evolution based on precipitate evolution during processing for predicting the steady-state creep rate. A similar approach is adapted utilizing precipitation simulations, but which include the effect of precipitate coarsening during long-term exposure at high temperature during use, as well as vacancy diffusivity as function of alloy composition. These additions are not limited to the currently selected model, but can be utilized for any preferred mechanism-based flow-stress or creep rate model. This allows for extended predictive capabilities to evaluate the influence of thermal history and alloy composition on the predicted creep behaviour, enabling chemistry optimization and design of novel chemistries with improved and tailored properties.

2.2 Modelling microstructure evolution using CALPHAD tools

A generic composition of alloy IN718 was defined as the following, in mass-%: Ni-19Cr-17Fe-5Nb-3Mo-0.9Ti-0.5Al. Thermodynamic calculations and kinetic simulations were performed using the Thermo-Calc software package (Andersson *et al.*, 2002), version 2021b and the TCNI11 and MOBNI5 Ni-base alloy thermodynamic and kinetic databases. This includes simulations using the Precipitation Module (TC-PRISMA). For each TC-PRISMA simulation, model parameters were selected or calibrated to available experimental data and based on existing knowledge and metallurgical understanding about the microstructure evolution, aiming for an overall robust fit ultimately capturing the concurrent precipitation and coarsening of the different precipitate phases.

The alloy was considered to be metastable, including primarily the phases FCC_A1 (γ), FCC_L12 (γ') and Ni3Nb (γ''). The stable Ni3Nb (δ) phase was also included in the creation of a Time-Temperature-Transformation (TTT) diagram, which was used to determine the sensitivity of the final microstructure to process variations, as a means to select relevant phases in the microstructure evolution modelling. Input parameters including nucleation site density and interfacial energy were tuned until early-stage precipitation matched experimental observations, in order to obtain TTT curves of initial transformation. The input parameters used for the TTT diagram calculations are listed in Table 1. For the γ' phase, a linearly decreasing interfacial energy, as a function of temperature, was adopted, fitted to the abovementioned coarsening data

at two different temperatures, as well as an arbitrary value in order to stabilize it at higher temperature. Both γ'' and γ' used the nucleation sites calculated from the matrix phase dislocation density, given as $5 \cdot 10^{11}$, which is one order of magnitude lower than default. The matrix phase elastic property defaults were used (i.e. 232.5, 136.6 and 120 GPa for c_{11}, c_{12} and c_{44} respectively), as well as the default grain size of 100 µm.

At longer treatment times of alloy 718, eventually the metastable γ'' phase transforms into the stable δ phase. This mechanism is not implemented in the TC-PRISMA software, therefore the nucleation site density of δ precipitates can be arbitrarily selected. However, since δ is known to form from γ'', the calculated number density after simulated two-stage annealing (in the order of 10^{22}) is an upper bound for reasonable nucleation site density values. Additionally, since the simulation immediately begins precipitating δ, a significantly lower value must be used to delay the δ formation, in accordance with experimental TTT curves, in this case 10^{20} was used. The interfacial energy was adjusted in order to promote the formation of δ in a reasonable temperature range. This resulted in a linearly decreasing interfacial energy, as given in Table 2.

Table 1: TC-PRISMA settings used for IN718 TTT diagram calculations

Phase	Elastic properties	Grain size	Interfacial energy σ	Aspect ratio	Morphology	Transformation strains	Nucleation site density
Matrix	c11=225 c12=110 c44=57	60 µm					N/A
γ'			0.047 -3.4E-5*T		Spherical	Calculated from molar volume	Calc. from matrix dislocation density
γ''			0.016	5	Plate	ε11 = 0.00667 ε22 = 0.00667 ε33 = 0.0286	Calc. from matrix dislocation density
δ			0.21 -1.1E-4*T	5	Plate	Ignored	1e20

To provide a more realistic as-processed microstructure prediction, a typical two-stage precipitation annealing followed by a 10 000-hour heat treatment at an elevated temperature was simulated using TC-PRISMA. The settings used in the TC-PRISMA simulation for the matrix phase and the individual precipitates are given in Table 2. These parameters were adjusted to fit experimental coarsening data up to 300 hours (Han, Deb and Chaturvedi, 1982; Sundararaman, Mukhopadhyay and Banerjee, 1992; Devaux *et al.*, 2008; Wu, Chen and Mason, 2018), for more accurate predictions of long-term precipitate evolution. This fit can be seen in figures A1 and A2 in the APPENDIX 1 – Supplementary figures.

Table 2: TC-PRISMA settings for phases included in coarsening simulation

Phase	Elastic properties	Grain size	Interfacial energy σ	Aspect ratio	Morphology	Transformation strains
Matrix	c11=225.0412 c12=110.8412 c44=57.1	60 µm				
γ'			0.012		Spherical	Calculated from volume
γ''			0.016	4.5	Plate	ε11 = 0.00667 ε22 = 0.00667 ε33 = 0.0286

2.3 Strength modelling

Strength is determined by a combination of strength contributions, including Hall-Petch strengthening, solution strengthening and precipitation strengthening. In this paper, the focus is on precipitation strengthening, σ_P, and how it evolves with time and temperature during IN718 processing condition and in-service use. The competing mechanisms of precipitate strengthening in alloy 718 are bowing (Orowan strengthening, σ_{Oro}) and coherency-dominated shearing (coherency strengthening, σ_{Coh}), thus, in this paper we use equation 2 below. It is important to note that while other strengthening contributions are non-negligible, IN718 belongs to the class of precipitate-strengthened alloys, where precipitate strengthening is the most important contribution to the strength.

$$\sigma_P = \min(\sigma_{Oro}, \sigma_{Coh}) \qquad (2)$$

Where, σ_{Oro} is calculated according to Brown and Ham (Brown, L. M.; Ham, 1971), and σ_{Coh} is given by the model from Gerold and Haberkorn (Gerold and Haberkorn, 1966). Detailed description of the different sub-models is available in a paper by Ahmadi et al. (Ahmadi *et al.*, 2014).

The strength modelling is used for stand-alone strength predictions, and also to provide input for the creep model framework in order to connect creep rate and microstructure evolution. σ_P is the main parameter in the model used to describe the power-law breakdown parameter P in equation 1, and σ_{Oro} is a key parameter in the prediction of the threshold stress evolution which is included in σ_{eff}.

2.4 ICME-guided alloy design

The unique aspect of ICME is the use and integration of computational tools and physics-based models at different time- and length-scales to predict the microstructure or property evolution of a material for engineering purposes. By combining results such as those presented herein, with relevant processing- and performance simulation tools and numerical models, location-specific properties can be predicted as well as performance variations with uncertainty quantification (QuesTek Innovations LLC, 2020).

In the example of aeroengine components, the peak stress and temperature may be localized, causing excessive damage to the most exposed parts of the blades and disks. Assuming that a component has been designed using a maximum load of 750 MPa at 600 ºC, the expected time-to-rupture is around 1000h (Brinkman, Booker and Ding, 2012), however, if the thermal barrier coating or the cooling system fails, and the maximum local

temperature is increased to 700 ºC, the component may fail already after a few hours. In addition to careful component and system design, another venue to improve performance is chemistry optimization or alloy design.

While Eq. 1 is a full model for creep rate with fitting parameters for a variety of mechanisms, vacancy diffusivity is a specific parameter that controls both coarsening of precipitates and dislocation movement. With the state-of-the-art mobility database for multicomponent Ni alloys, we can calculate, rather than fit, the vacancy diffusivity given the matrix composition. This in turn allows predictions beyond experimental data sets. Such examples are presented herein, and how they can be used for chemistry- and performance optimization purposes.

3.0 RESULTS

The CALPHAD-based tools and associated databases have been used for simulation of strengthening precipitates in IN718 during two-stage annealing followed by long-term ageing at 600 and 800 ºC, as well as to predict a TTT diagram. The resulting data on precipitate size with time and temperature have been further used in mechanistic strength and creep modelling framework to predict creep performance.

3.1 Microstructure evolution during processing

A critical step towards predicting and potentially enhancing component lifetime is to accurately control the microstructure of the material in the as-processed state. Here we present example simulations of the microstructure evolution of alloy 718 during precipitation heat treatment of a homogenized material.

Figure 4 presents a simulated TTT diagram, with experimental TTT curves in the background, which have been digitized from known diagrams in literature (Keiser and Brown, 1976; Brooks and Bridges, 1988; Oradei-Basile and Radavich, 1991). Large discrepancies between the different TTT diagrams are seen, thus large uncertainties are expected. Brooks was the only one to separate the precipitation of γ'' and γ', whereas the other two combine the two precipitates in the same region. Furthermore, Brooks separated the onset of grain boundary δ precipitation and bulk δ precipitation; the present work did not obtain satisfactory results when including grain boundary δ precipitation, since this is a different precipitation mechanism that is challenging to include at the same time as the other precipitates. Nevertheless, the present results show the possibility to use CALPHAD-based simulations to evaluate the process sensitivity of the material microstructure, which in turn may be used to evaluate property and performance variability due to process adjustments.

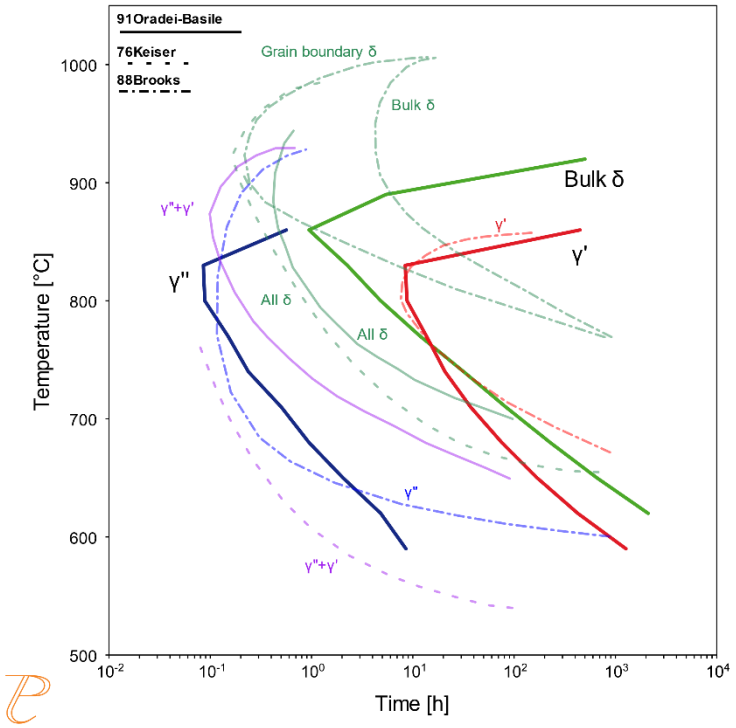

Figure 2: Simulated TTT-diagram for a completely solutionized alloy 718 compared to experimental data from literature (Keiser and Brown, 1976; Brooks and Bridges, 1988; Oradei-Basile and Radavich, 1991)

Similarly, the precipitation during a specific processing route can be predicted based on appropriate time-temperature profiles. Here a common two-step annealing of alloy 718 is simulated, providing insight into how the volume fraction and size of the main strengthening precipitate γ'', as well as γ', evolve during the processing steps (see Figures 3 a and b). Figure 3a presents the increasing volume fractions of the precipitates, and evidently the simulation predicts a very fast initial precipitation. After the treatment, there is about double the amount of γ'' as γ'. In this figure, the two temperature stages are overlain. Figure 3b presents the increasing mean precipitate sizes during the treatment, and shortly after reaching the second temperature step the mean sizes increase rather slowly. This predicted microstructure is hence used as the starting point for strength modelling and simulations of microstructure evolution during prolonged high-temperature exposure.

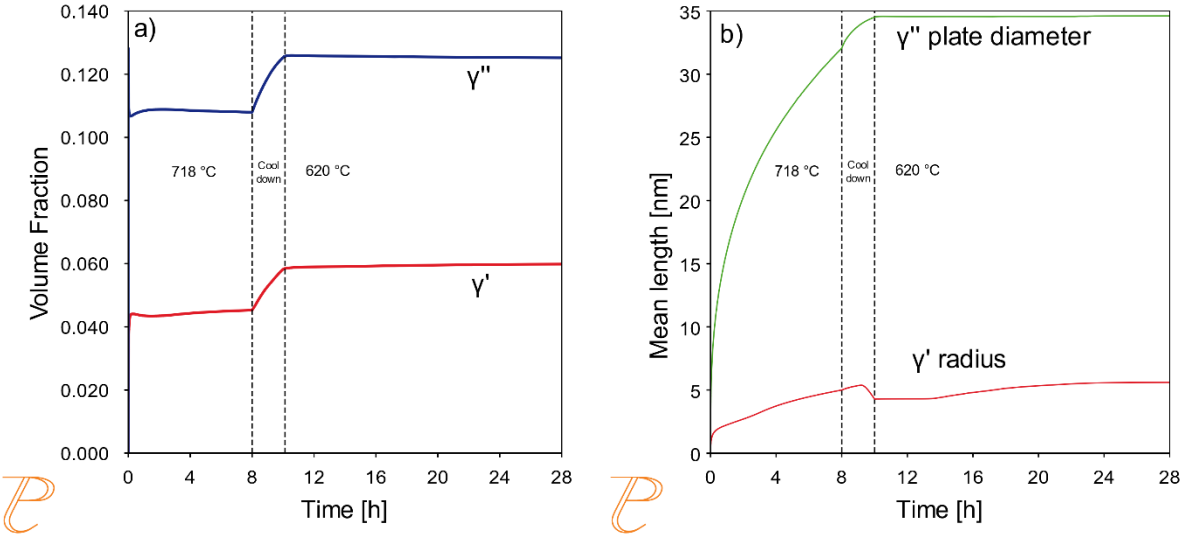

Figure 3: Simulated precipitate a) volume fraction and b) size evolution during the two-step annealing

3.2 Microstructure and property evolution during application

Microstructure evolution is one of the sources of changing / decreasing mechanical properties during application at high temperatures. In case of IN718, excellent mechanical properties are maintained for long times up to approximately 650 ºC, but quickly deteriorate at higher temperatures (Cozar and Pineau, 1973; Azadian, 2004; Manriquez *et al.*, 2012). As seen in the TTT diagram, more than 1000h of isothermal annealing is required to precipitate delta-phase at 650 ºC, whereas it appears within an hour when annealing at higher temperatures.

3.2.1 γ'' evolution below and above standard operating temperature limit

The coarsening of the main precipitates γ'' and γ' were simulated for 10 000 hours at 600 ºC, below, and at 800 ºC, above standard operating temperature limits for IN718. Figures 4a and 5a show how the precipitate volume fractions evolve during those treatments, and figures 4b and 5b show how the precipitate mean size develop. What is most alarming about the results is that at 800 ºC the size of the precipitates after the long treatment is tenfold that of the 600 ºC treatment. Furthermore, as the metastable equilibrium phase fractions of the precipitates are lower closer to the solvus temperatures, the volume fraction of precipitates is drastically lower after prolonged exposure at 800 ºC compared with 600 ºC.

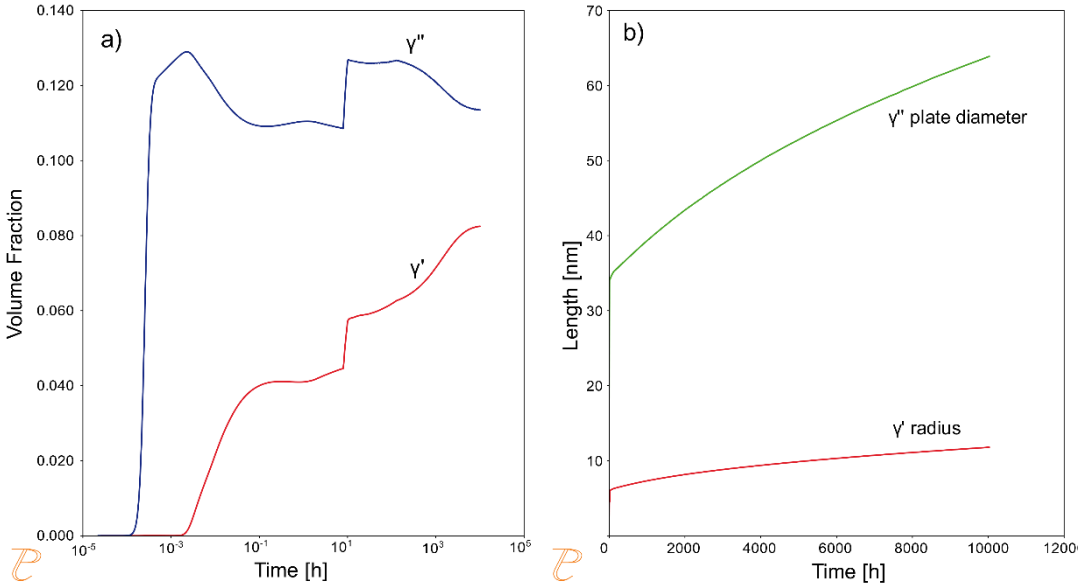

Figure 4: Simulated a) volume fraction, and b) size of γ' and γ'' precipitates during long exposure at 600 ºC

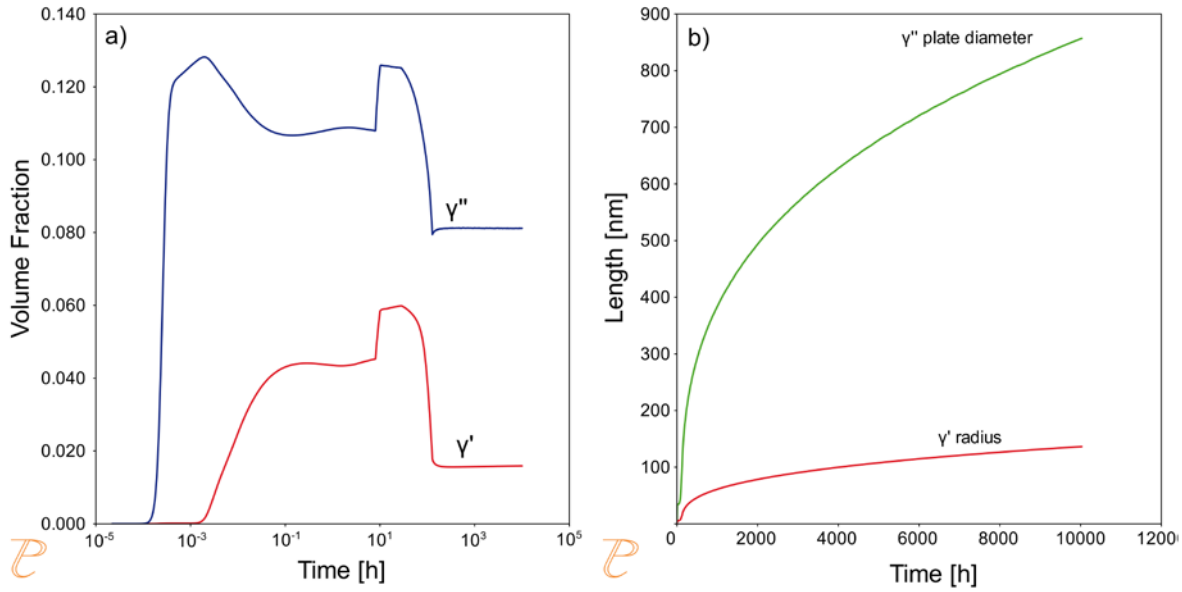

Figure 5: Simulated a) volume fraction, and b) size of γ' and γ'' precipitates during long exposure at 800 ºC

3.2.2 Strength and strain rate evolution during high-temperature exposure

Based on the simulated precipitate coarsening in Figures 4 and 5, the corresponding loss in yield strength is calculated using the strength model. As clearly seen in Figure 6a, the strength at 600 ºC is relatively stable up to 1 000 h exposure, while at 800 ºC there is a drastic drop in strength already after 100 h. By incorporating this computationally predicted yield strength as function of time in the creep modelling framework, the progressive deterioration of the material microstructure and properties is reflected in the creep strain rate calculations, see Figure 6b. By combining this type of modelling with measured or simulated temperature and

stress distributions in an aeroengine component, it would be possible to evaluate the location-specific lifetime for given operational conditions.

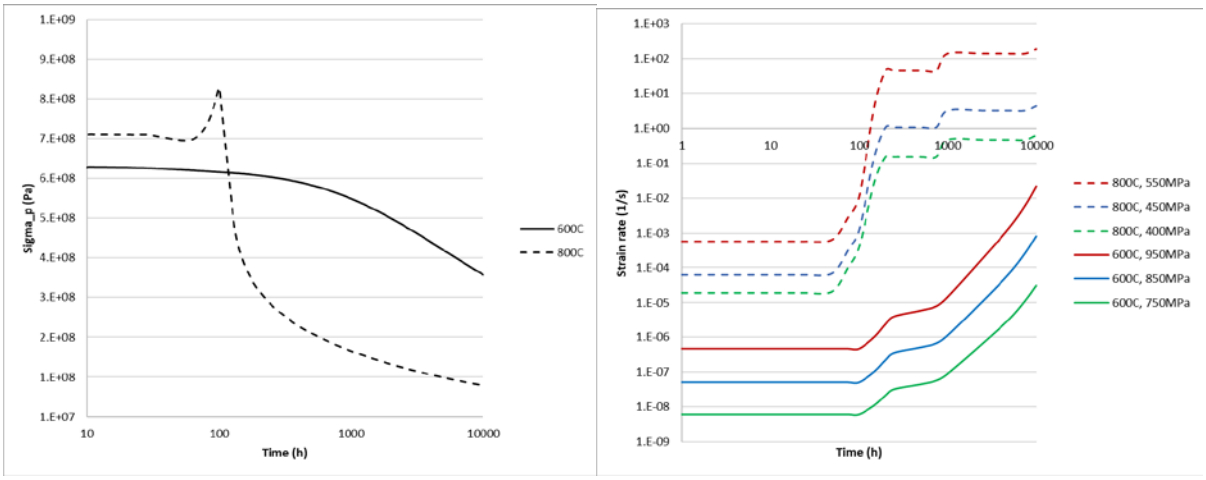

Figure 6: a) (left) Calculated precipitate strengthening evolution at 600 and 800 ºC due to γ'' precipitate coarsening and dissolution, and b) (right) calculated creep strain rate at 600 and 800 ºC with varying applied stress.

3.3 CALPHAD-enhanced creep life predictions and alloy design

The drastic changes in strain rate associated with microstructural changes clearly show the importance of microstructural control, not only for process design but also for alloy design for long-term creep performance. With the model parameters for the physics-based creep model determined using CALPHAD, the physically significant model parameters can be used as design metrics, as exemplified below.

The microstructural evolution of the alloy as shown in Figures 4 and 5 can be parameterized into equilibrium precipitate volume fraction and precipitate coarsening rate. In addition to these microstructural stability metrics, and their effect on the strength evolution of the alloy, the creep behaviour described by equation 1 is sensitive to the vacancy diffusivity. All of these metrics can be calculated using CALPHAD-based tools to account for any composition dependence, and could thus be used in a parametric materials design approach upon quantification of their design minimums. Figure 7a exemplifies the influence of Cr and Fe content on vacancy diffusivity and γ'' coarsening rate of alloy IN718 beyond its nominal composition.

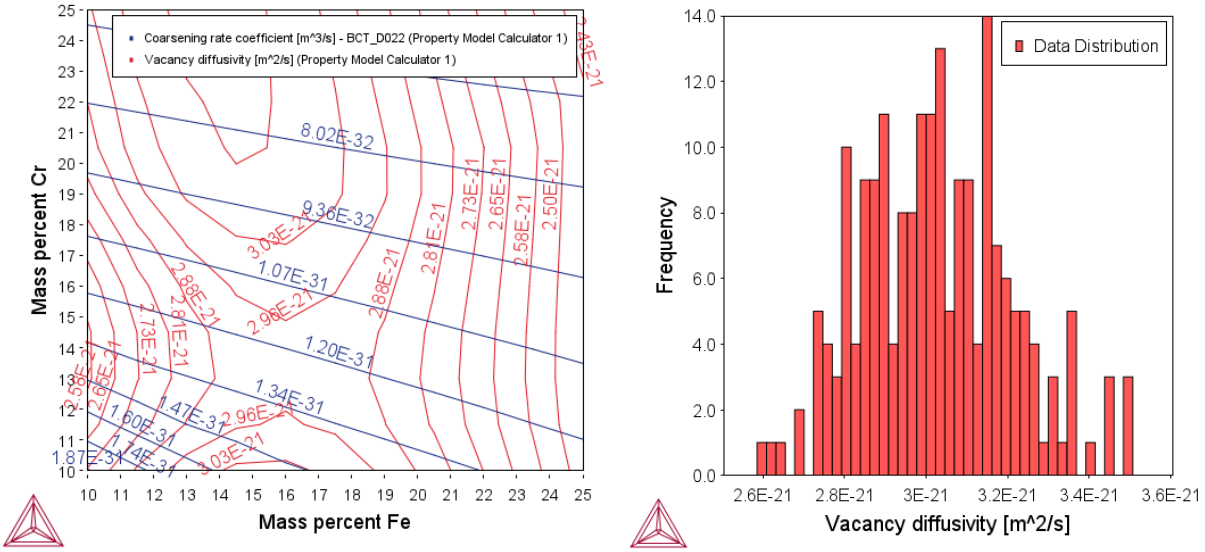

Figure 7: a) Influence of Cr and Fe content on the vacancy diffusivity in the matrix (red) and y'' coarsening rate (blue) of alloy 718 at 600 ºC, and b) calculated variation of vacancy diffusivity within 718 alloy specification.

Similarly, the sensitivity of design parameters on composition variations within alloy specification can be useful in quantifying alloy creep performance variability. Figure 7b shows the frequency distribution of the vacancy diffusivity within the full IN718 specification. The corresponding effect on creep strain is shown in Figure 8. In Figure 8, the black line corresponds to the nominal vacancy diffusivity for an alloy with nominal composition, while the max. (+38% from nominal D_{vac}) and min. (-28% from nominal D_{vac}) values are extracted from the variations within the alloy specification. Such data can be utilized when generating or modifying a material specification, where it is critical to account for maximum allowable performance variations within a composition range. Additionally, by utilizing CALPHAD-based material parameters in lifetime predictions, the component design criteria may be evaluated on a supplier-to-supplier basis, which could help ensure consistent part performance. Furthermore, given the specific chemistry range of a batch of components, the lifetime variability may even be estimated using batch-specific model parameters instead of the traditionally used constant fitting parameters, potentially reducing necessary safety margins. Once validated for a specific industrial process, this CALPHAD-based modelling approach may contribute to optimization of maintenance schedules for each specific batch of components.

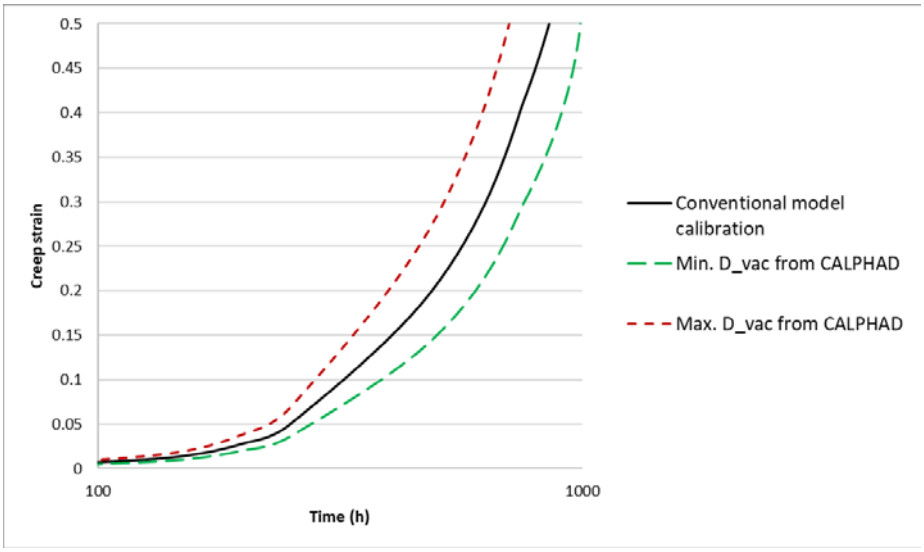

Figure 8: Influence of composition-induced variation of vacancy diffusivity on the calculated creep curve at 600ºC and 850 MPa.

These examples assume no other influence on the microstructure of IN718; however, similar parametrization and calculations can be performed on other critical materials design metrics, such as corrosion resistance, in order to identify compositions that meet all property criteria for the intended application. This would then allow for tailored alloy design and accelerated development of new materials for further performance enhancement.

4.0 SUMMARY AND CONCLUSION

This paper has exemplified an ICME-based approach to predicting elevated temperature creep rate in Ni superalloys using CALPHAD-based microstructure evolution simulations. The use of specific CALPHAD-based tools for understanding and predicting the microstructure evolution of materials is shown, exemplified by IN718, during alloy processing and in-service use. Specifically, TC-PRISMA precipitation simulations are used to provide input for a strength model to calculate threshold stress, based on the presence of primary and secondary precipitates evolving with time and temperature. These predictions combined with vacancy diffusivities determined creep rate across time, temperature and stress, ultimately simulating an aeroengine component in-service. The effect of chemistry variation, within and outside IN718 specification, on diffusivity and its corresponding effect on creep strain was exemplified, to show how computational thermodynamics and kinetics can be used to increase the predictive capabilities of existing material models beyond well-studied composition spaces. By integrating CALPHAD-based tools and predictions in an ICME framework it is possible to move beyond empirical modelling and data fitting, to physics-based and predictive modelling of composition variations and microstructure evolution, ultimately enabling novel alloy design with improved performance.

REFERENCES

Ahmadi, M. R. *et al.* (2014) 'Yield strength prediction in Ni-base alloy 718Plus based on thermo-kinetic precipitation simulation', *Materials Science and Engineering: A*, 608, pp. 114–122. doi: 10.1016/j.msea.2014.04.054.

Andersson, J. O. *et al.* (2002) 'Thermo-Calc & DICTRA, computational tools for materials science', *Calphad: Computer Coupling of Phase Diagrams and Thermochemistry*. doi: 10.1016/S0364-5916(02)00037-8.

Azadian, S. (2004) *Aspects of Precipitation in Alloy Inconel 718*. Lund tekniska universitet. Available at: http://www.diva-portal.org/smash/record.jsf?pid=diva2%3A999089&dswid=-3604.

Brinkman, C. R., Booker, M. K. and Ding, J. L. (2012) 'Creep and Creep-Rupture Behavior of Alloy 718', in. doi: 10.7449/1991/superalloys_1991_519_536.

Brooks, J. W. and Bridges, P. J. (1988) 'Metallurgical Stability of Inconel Alloy 718', in *Superalloys 1988 (Sixth International Symposium)*. TMS, pp. 33–42. doi: 10.7449/1988/Superalloys_1988_33_42.

Brown, L. M.; Ham, R. K. (1971) 'Dislocation-particle interactions', in Kelly, A.; Nicholson, R. B. (ed.) *Strengthening Methods in Crystals*. London, UK: Applied Science Publishers LTD, pp. 9–135.

Cozar, R. and Pineau, A. (1973) 'Morphology of y' and y" precipitates and thermal stability of inconel 718 type alloys', *Metallurgical Transactions*. doi: 10.1007/BF02649604.

Devaux, A. *et al.* (2008) 'Gamma double prime precipitation kinetic in Alloy 718', *Materials Science and Engineering: A*, 486(1–2), pp. 117–122. doi: 10.1016/j.msea.2007.08.046.

Drexler, A. *et al.* (2015) 'Yield stress evolution in Inconel 718 samples under standard heat treatment process conditions of turbine disks', in *European Conference on Heat Treatment 2015 and 22nd IFHTSE Congress - Heat Treatment and Surface Engineering from Tradition to Innovation*.

Drexler, A. *et al.* (2018) 'A microstructural based creep model applied to alloy 718', *International Journal of Plasticity*, 105, pp. 62–73. doi: 10.1016/j.ijplas.2017.11.003.

Gerold, V. and Haberkorn, H. (1966) 'On the Critical Resolved Shear Stress of Solid Solutions Containing Coherent Precipitates', *physica status solidi (b)*, 16(2), pp. 675–684. doi: 10.1002/pssb.19660160234.

Gibbs, J. W. (1873) 'A Method of Geometrical Representation of the Thermodynamic Properties of Substances by Means of Surfaces', *Transactions of the Connecticut Academy*, II, pp. 382–404. Available at: https://en.wikisource.org/wiki/Scientific_Papers_of_Josiah_Willard_Gibbs,_Volume_1/Chapter_II.

Han, Y., Deb, P. and Chaturvedi, M. C. (1982) 'Coarsening behaviour of γ″- and γ′-particles in Inconel alloy 718', *Metal Science*, 16(12), pp. 555–562. doi: 10.1179/030634582790427118.

Heilmaier, M. and Reppich, B. (1999) 'Particle Threshold Stresses in High Temperature Yielding and Creep : a Critical Review', *Creep Behavior of Advanced Materials for the 21st Century*.

Keiser, D. D. and Brown, H. L. (1976) 'A Review of the Physical Metallurgy of Alloy 718', *Aero Jet Nuclear Company*, (February).

Li, Y. and Langdon, T. (1997) 'A simple procedure for estimating threshold stresses in the creep of metal matrix composites', *Scripta Materialia*, 36(12), pp. 1457–1460. doi: 10.1016/S1359-6462(97)00041-9.

Liu, W. C., Yao, M. and Chen, Z. L. (1999) 'Effect of cold rolling on the precipitation behavior of δ phase in INCONEL 718', *Metallurgical and Materials Transactions A*, 30(1), pp. 31–40. doi: 10.1007/s11661-999-0193-7.

Lukas, H., Fries, S. G. and Sundman, B. (2007) *Computational Thermodynamics*, *Computational Thermodynamics*. doi: 10.1017/cbo9780511804137.

Malmelöv, A. *et al.* (2020) 'Mechanism Based Flow Stress Model for Alloy 625 and Alloy 718', *Materials*, 13(24), p. 5620. doi: 10.3390/ma13245620.

Manriquez, J. A. *et al.* (2012) 'The High Temperature Stability of IN718 Derivative Alloys', in. doi: 10.7449/1992/superalloys_1992_507_516.

Oradei-Basile, A. and Radavich, J. F. (1991) 'A Current T-T-T Diagram for Wrought Alloy 718', in *Superalloys 718, 625 and Various Derivatives (1991)*. TMS, pp. 325–335. doi: 10.7449/1991/Superalloys_1991_325_335.

QuesTek Innovations LLC (2020) *QuesTek Wins Air Force Research Lab Additive Manufacturing Modeling Challenge*. Available at: https://www.questek.com/2020/07/28/questek-wins-air-force-research-lab-additive-manufacturing-modeling-challenge/ (Accessed: 3 September 2021).

Sundararaman, M., Mukhopadhyay, P. and Banerjee, S. (1992) 'Some aspects of the precipitation of metastable intermetallic phases in INCONEL 718', *Metallurgical Transactions A*, 23(7), pp. 2015–2028. doi: 10.1007/BF02647549.

Wilshire, B.; Evans, R. W. (1985) *Creep behaviour of crystalline solids*. Pineridge Press, University of California.

Wu, K., Chen, Q. and Mason, P. (2018) 'Simulation of Precipitation Kinetics with Non-Spherical Particles', *Journal of Phase Equilibria and Diffusion*, 39(5), pp. 571–583. doi: 10.1007/s11669-018-0644-1.

APPENDIX 1 – Supplementary figures

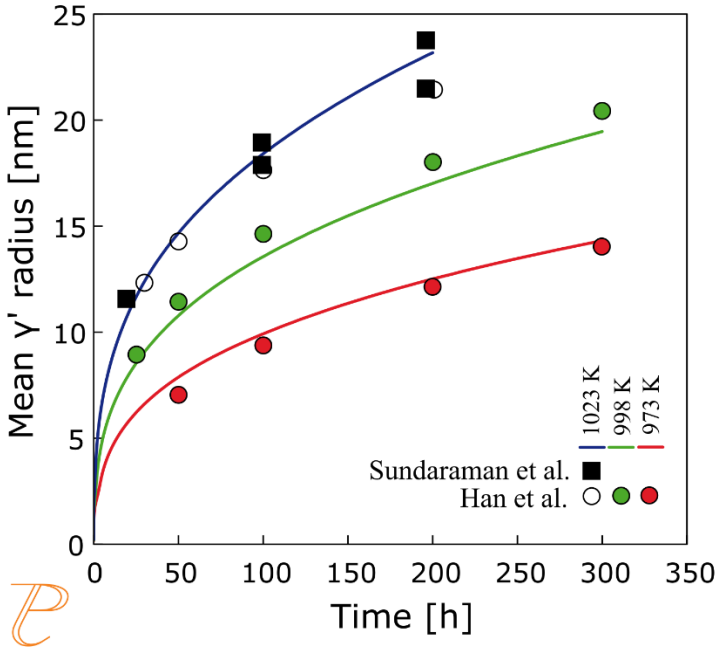

Figure A1: γ' precipitate radius compared with literature data, during long annealing at different temperatures

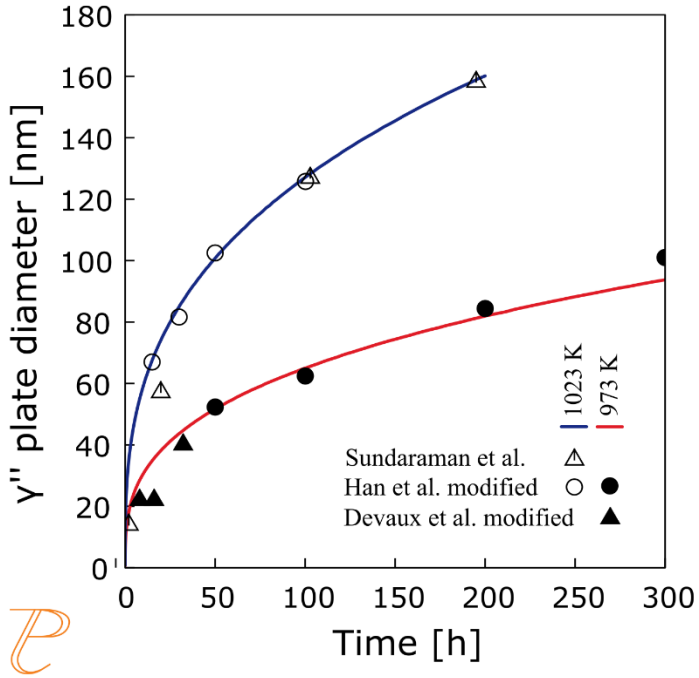

Figure A2: γ'' plate diameter compared with literature data, during long annealing at different temperatures